Disorder and ferromagnetism in diluted magnetic semiconductors

S.-R. Eric Yang[1,2] and A. H. MacDonald[2]
[1]*Department of Physics, Korea University, Seoul 136-701, Korea*
[2]*Department of Physics, University of Texas at Austin, Austin, Texas 78712*
(Received 9 December 2002; published 2 April 2003)

We have investigated the interplay between disorder and ferromagnetism in $III_{1-x}Mn_xV$ semiconductors. Our study is based on a model in which $S=5/2$ Mn local moments are exchange coupled to valence-band holes that interact via Coulomb interactions with each other, with ionized Mn acceptors, and with the antisite defects present in these materials. We find quasiparticle participation ratios consistent with a metal-insulator transition that occurs in the ferromagnetic state near $x\sim 0.01$. By evaluating the distribution of exchange mean fields at Mn moment sites, we provide evidence in favor of the applicability of impurity-band magnetic-polaron and hole-fluid models on insulating and metallic sides of the phase transition, respectively.

DOI: 10.1103/PhysRevB.67.155202 PACS number(s): 75.50.Pp, 75.10.−b, 75.30.Hx, 73.21.−b

I. INTRODUCTION

Recent progress[1] in the growth of diluted magnetic semiconductors that exhibit ferromagnetism[2] at relatively high temperatures has suggested exciting new possibilities for devices that combine information processing and storage functionalities in a single material. It is generally accepted[3] that Mn acts as an acceptor in these semiconductors, that its half-filled *d* shell contributes a $S=5/2$ local moment[4–6] to the system's low-energy degrees of freedom, and that ferromagnetism is due to the interactions between local moments that are mediated by valence-band holes. Recent experiments[7–10] demonstrate that ferromagnetism occurs in both metallic and insulating states, and that both magnetic and transport properties are sensitive to the Mn fraction *x* and to the density of compensating antisite and other defects in the material. The highest ferromagnetic critical temperatures T_c appear[10] to occur in the most metallic samples. The role of Coulomb interactions in the ferromagnetism in these materials is subtle. At high carrier densities, well on the metallic side of the metal-insulator transition, exchange and correlation in the hole system is expected[11] to enhance ferromagnetism. Well on the insulator side of the transition, however, Coulomb interactions lead to a Mott gap that increases the importance of randomness in Mn ion positions, suppresses carrier hopping between Mn sides, and eventually turns off the coupling between local moments that can lead to ferromagnetism.

In this paper, we report on a numerical Hartree-Fock study of model (III,Mn)V ferromagnets in both metallic and insulating regimes. By evaluating the distribution of $T=0$ Mn exchange mean fields, defined precisely below, we find evidence that is generally supportive of the impurity-band magnetic-polaron[12–14] picture that has been used to describe ferromagnetism in the insulating regime, and of the hole-fluid picture that has been used[3,11,15,16] in the metallic regime. The objective of this numerical study is to provide a basis for qualitative judgments on the applicability of simplified models that are often applied far in one regime or the other, not to explore the physics of the transition itself.

Our principle results are summarized in Fig. 2 where we plot the fraction of Mn sites that have exchange mean-fields larger than k_BT, vs *T*. In the metallic case[17] ($x=0.05$ and hole density $n_h=3.3\times10^{20}$ cm^{-3}) the distribution of coupling strengths is peaked at a finite value close to its uniform hole-fluid value and all Mn ions are strongly coupled to holes. In the insulating case ($x=0.01$ and hole density $n_h=2.8\times10^{19}$ cm^{-3}), on the other hand, we find that the vast majority of Mn spins are nearly free; the few strongly coupled Mn ions form magnetic polarons that grow slowly in size and interact more strongly as the temperature is lowered. In the following sections we explain how these results were obtained and elaborate on their significance for models of diluted magnetic semiconductor ferromagnetism. In Sec. II, we discuss the partly phenomenological model Hamiltonian that we use, emphasizing some assumptions that are implicit in its use. In Sec. III, we discuss our numerical results more fully. An important conclusion of this work is that Coulomb interactions must be included in order to obtain a reasonable description of the localized quasiparticle states that occur when the free carrier density is low and play an increasingly important role as disorder increases.

II. MODEL HAMILTONIAN

Most theoretical work on (III,Mn)V ferromagnets has started from one of two idealized limits. Impurity-band models[12–14] achieve simplification by assuming that the holes that mediate interactions between Mn ion moments are strongly localized, whereas hole-fluid models achieve simplification by neglecting disorder due to Mn acceptors and other defects and treating it perturbatively in estimating transport coefficients. An insulator to metal phase transition occurs in these ferromagnets as Mn and hole densities increase; experimentally[1] it appears that the metal-insulator transition usually occurs near $x\sim0.01$, likely depending on the density of compensating antisite defects, a quantity that is expected to be sensitive to the details of sample growth and annealing protocols. Although it is generally agreed that an impurity band picture should apply far on the insulator side of the transition and a hole-fluid model far on the metallic side of the transition, it has not been clear which approach is a better starting point in the experimentally relevant parameter ranges. We address this issue by examining the ferromag-

netic ground state using a model, and an approximation scheme, that captures the physics of both limits correctly and can be applied at intermediate parameter values. Our study is built on $\vec{k}\cdot\vec{p}$ envelope-function approach description of the valence band[18] and a Hartree-Fock description of interactions.

The four terms in the single-particle part of our band electron model Hamiltonian, $H^0=H^K+H^{K.ex.}+H^{Mn-h}+H^{as-h}$, require some discussion. $H^{K.ex.}$ represents the kinetic exchange interaction between band electrons and Mn local moments, assumed to be aligned in the ferromagnetic system ground state,[19] H^{Mn-h} represents the attractive Coulomb interaction between an ionized Mn^{2+} acceptor and a valence-band hole. In an envelope function formalism, central cell corrections to this interaction are necessary[20] to achieve an accurate description of the isolated bound-acceptor limit. H^{as-h} describes the repulsive interaction between holes and antisite defects (represented as sites with charge $+2$). These defects act as deep donors partially compensating the Mn acceptors and reducing the overall hole density, and provide an important additional scattering center. H^K is the usual kinetic energy term. In this study we ignore[8,16,21] mixing between heavy- and light-hole bands by using a simple parabolic band approximation.

$$H^0=\frac{-\hbar^2}{2m}\vec{\nabla}+\frac{1}{2}S\sum_I \hat{\Omega}_I\cdot\vec{\tau}J(\vec{r}-\vec{R}_I) + \sum_I\left(-\frac{e^2}{\epsilon|\vec{r}-\vec{R}_I|}-V_0e^{-|\vec{r}-\vec{R}_I|^2/r_0^2}\right)+\sum_K\frac{2e^2}{\epsilon|\vec{r}-\vec{R}_K|}. \tag{1}$$

Here $J(\vec{r})=[J_{pd}/(2\pi a_0^2)^{3/2}]\exp(-r^2/2a_0^2)$, $\vec{\tau}=(\tau_x,\tau_y,\tau_z)$ is the Pauli spin matrix vector, I labels Mn sites, K labels antisite defect sites, and $\hat{\Omega}_I$ is the orientation of the Ith Mn spin. The term in the potential proportional to V_0 is a central cell correction discussed below. Both Mn ions and antisites were distributed randomly[22] in a cube of side L. The long range of the Coulomb interaction requires overall charge neutrality so that $n_h-N_{Mn}+2N_{as}=0$, where N_{Mn} the density of Mn ions and N_{as} the density of antisites. In the ground state, all Mn spins are oriented along the $\hat{z}$ direction and H^0 is block diagonal in its spin indices. In the spin-wave configurations discussed below, both $\hat{x}$ and $\hat{y}$ components of the spins are present, doubling the dimension of the matrix that must be diagonalized numerically. The wave-vector cutoff in the quasiparticle wave-function expansion[23] was tested by computing the binding energy of a hole to an isolated Mn, comparing with the results of Bhattacharjee and Benoit a la Guillaume[20] who find that a binding energy of 112 meV, 86 meV when the kinetic exchange term is neglected, and 68 meV when the central cell correction is also neglected. Our results are 124 meV, 88 meV, and 48 meV, respectively, demonstrating an adequate description of the completely isolated Mn limit.

In order to capture the correct physics of both metallic and impurity band limits, hole-hole interactions must be described using an approximation that accounts for screening effects in the metallic regime and avoids artificial self-interaction effects in the localized regime, motivating our use of Hartree-Fock (HF) theory.[24] The HF quasiparticle Hamiltonian is $H^{HF}=H^0+(V^H+V^X)$ where

$$V^H_{\vec{k}\sigma,\vec{k}'\sigma'}=\delta_{\sigma,\sigma'}\sum_{\sigma''}\sum_{\vec{p}}\frac{4\pi e^2}{\epsilon|\vec{k}-\vec{k}'|^2}\rho_{\vec{p}\sigma'',\vec{k}'+\vec{p}+\vec{k}\sigma''} \tag{2}$$

and

$$V^X_{\vec{k}\sigma,\vec{k}'\sigma'}=-\sum_{\vec{p}}\frac{4\pi e^2}{\epsilon|\vec{k}-\vec{p}|^2}\rho_{\vec{p}\sigma,\vec{k}'-\vec{k}+\vec{p}\sigma'} \tag{3}$$

are the Hartree and Fock contributions. These interaction contributions to the Hamiltonian must be evaluated self-consistently and are expressed above in terms of the $\vec{k}$-space representation for the density matrix that we use to expand our envelope function quasiparticle wave functions: $\rho_{\vec{k}\sigma,\vec{k}'\sigma'}=\Sigma_\alpha n_\alpha c^{(\alpha)}_{\vec{k}\sigma}c^{(\alpha)*}_{\vec{k}'\sigma'}$, where $|\alpha\rangle=\Sigma_{\vec{k}\sigma}c^{(\alpha)}_{\vec{k}\sigma}|\vec{k}\sigma\rangle$, and n_α is a quasiparticle occupation number. The quasiparticle energies thus include exchange contributions, so that the band minimum is shifted well below zero, even in the absence of disorder. Our HF scheme becomes *exact* in the strongly localized limit, since a localized quasiparticle does not interact with itself. It is expected to overestimate inhomogeneity in the metallic limit because it neglects quantum fluctuations in the many-hole state.

III. NUMERICAL RESULTS

A. Participation ratios

The HF scheme we employ is intended to model ferromagnetism in diluted magnetic semiconductors which has been observed for both localized and extended band quasiparticle wave functions. In order to verify that our model can correctly describe ferromagnetism on both sides of the metal-insulator transition and that the transition occurs near the same parameter range as in experimental systems, we measured the localization properties of our Hartree-Fock quasiparticles by evaluating their participation ratios, $P_\alpha=1/(L^3\int d^3r|\Psi_\alpha(\vec{r})|^4)$, where $\Psi_\alpha(\vec{r})=\langle\vec{r}|\alpha\rangle$ is a normalized quasiparticle wave function. [For a localized state $P_\alpha\sim(\xi_\alpha/L)^3$, where ξ_α is the localization length.] The antisite defects that appear because of the low-temperature MBE growth necessary to suppress MnV cluster formation play a very important role in (III,Mn)V ferromagnets, and are belived to be responsible for a high degree of compensation of Mn acceptors, especially at lower-Mn density. It is now[25,10] evident that the carrier density at a given Mn density, and consequently the ferromagnetic transition temperature and other magnetic properties, can be varied substantially by changing annealing conditions or even the thickness of the MBE grown film. We have performed numerical calculations for two cases. To represent typical metallic ferromagnets we consider the case $x\sim0.05$ and a ratio of hole to Mn density equal to 0.3. This compensation factor corresponds to that measured in typical *maximum* T_c samples as of about one

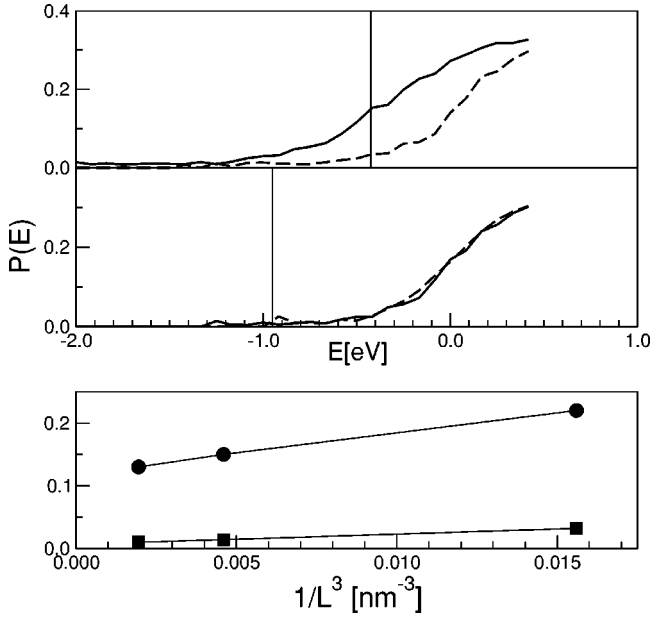

FIG. 1. Participation ratios vs energy in a simulation cell of side $L=8$ nm for majority (solid line) and minority (dashed lline) quasiparticles. The Fermi energies are indicated by solid vertical lines. (The choice of the zero of E is arbitrary). The upper panel is for the metallic case and the middle panel is for the insulating case. These results were obtained by averaging over 15 disorder realizations. The bottom panel shows the system size dependence of majority-spin participation ratios at the Fermi energy for the two cases.

year ago. More recently substantially higher carrier densities have been measured in suitably annealed samples with higher Mn fraction x that also have higher ferromagnetic transition temperatures and higher conductivities. These parameter values, which we refer to below as the *metallic* case, thus correspond to clearly metallic systems but not be any means to the maximum degree of metallicity that is currently achievable. To represent the case of $(III,Mn)V$ ferromagnetism in insulating samples, we have also studied the case $x\sim 0.0125$, assuming the higher degree of compensation that has been estimated for typical samples with this Mn fraction, $n_h=N_{Mn}/10$. Our results are plotted in Fig. 1. Note that for $x=0.05$ the participation ratios of the minority spins are significantly smaller than those of the majority spins, because of the smaller group velocities of the occupied states. The size dependence of the majority-spins Fermi-energy quasiparticle participation ratios are shown in the lowest panel of Fig. 1. The participation fractions extrapolated to infinite volume are clearly finite and therefore consistent with metallic transport at $x=0.05$, whereas they are consistent with zero and localized quasiparticles at $x=0.0125$, in agreement with the experiment. Experimentally, the transition between metallic and insulating ferromagnets occurs for $x\sim 0.02$, although this property is clearly also dependent on the degree of compensation.

B. Exchange coupling strength distribution

The exchange mean fields, used to construct Fig. 2, are given by $H_{eff,I}=\int d\vec{r} J(\vec{r}-\vec{R}_I)[n_\downarrow(\vec{r})-n_\uparrow(\vec{r})]/2 \approx J_{pd}[n_\downarrow(\vec{R}_I)-n_\uparrow(\vec{R}_I)]/2$, where the partial densities $n_{\uparrow,\downarrow}(\vec{r})$ are determined by solving the Hartree-Fock equations self-consistently. In the extreme impurity band limit, $H_{eff,I}$ would have the value $J_{pd}n_{max}/2\approx 25$ meV for a fraction n_h/N_{Mn} of the local moments, those on which a hole has localized, and much smaller values for all others. This estimate was obtained using for the maximum hole density n_{max} the value at the center of the roughly hydrogenic bound states for an isolated acceptor. (The shallow impurity Bohr radius a_B^* calculated using the heavy-hole mass is ~ 1.0 nm; the peak hole density, 4.9×10^{20} cm^{-3} is slightly larger than the shallow impurity value because of central cell corrections.) Our findings at $x=0.0125$ are in qualitative agreement with this expectation, although the maximum value of H_{eff} is somewhat smaller. There is no sharp peak in the distribution function near the peak value, presumably because of the variable Mn and antisite defect environment experienced by localized holes. Kaminski and Das Sarma[13] have recently estimated the impurity-band magnetic-polaron model T_c, relating it to N_{Mn}, n_h and the maximum mean-field exchange coupling by $T_c\sim 0.5(N_{Mn}/n_h)^{1/2}(n_h a_B^{*3})^{1/6}H_{max}\times\exp(-0.86/{n_h}^{1/3}a_B^*)/k_B$. Naively applying this formula to our $x=0.0125$ case using the shallow impurity Bohr radius yields $T_c\sim 15$ K, reasonably consistent with the values that are observed for these parameter values. Note that T_c is expected to decrease very rapidly at still smaller Mn fraction values as the overlap between holes bound to different Mn acceptors diminishes. The highest exchange coupling strengths in this case occur for the Mn spins on which the localized holes are centered. We note that the top 10% of exchange coupling strengths are those above a value that is smaller than H_{max} by more than a factor of two, i.e., above than ~ 13 meV~ 150 K. (Recall that the number of holes in this case is 10% of the number of Mn ions.) This numerical finding demonstrates that even for these parameter values, those at which the ferromagnetic transition temperature is already well below the relatively large values possible in the metallic regime, the typical hole localization length a_B^* is substantially larger than its dilute limit value. From these results we estimate an effective Bohr radius $a_B^*\sim 1.2$ nm, changing the naive T_c estimate only slightly to 30 K because the decrease in H_{eff} and the increase in a_B^* compared to the isolated limit cancel. The estimated T_c's are somewhat larger than what has typically been observed for strongly compensated samples at $x\sim 0.01$ in (Ga,Mn)As, possibly because the polaron theory neglects Pauli exclusion principle effects, superexchange interactions, that favor opposite orientations of nearby impurity-band holes and oppose ferromagnetism. Nevertheless, it appears from the distribution of exchange coupling strengths that the polaron picture provides a qualitative correct description of ferromagnetism for x less than about 0.01. This is true despite the absence of a clearly separated impurity band in the density of states curves shown in the inset of Fig. 2.

We note in particular that the concave $M(T)$ curves common in insulating examples are naturally explained[13] by wide variations in exchange coupling strengths. In the metallic case, for which the magnetization has a qualitatively differ-

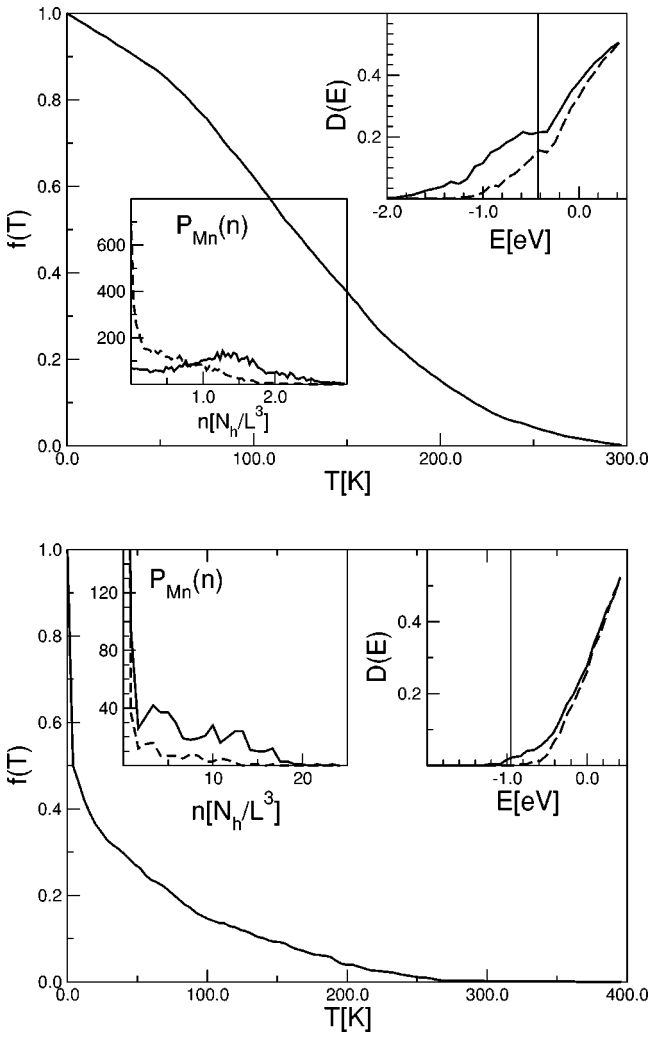

FIG. 2. Upper panel, $f(T)$, the fraction of Mn that experience a mean-field stronger than k_BT, vs T in the metallic case. ($N_{Mn}=1.0\ \mathrm{nm}^{-3}$, $n_h=N_{Mn}/3$.) $P_{Mn}(n)$, the probability distribution function for partial hole densities at Mn sites, is plotted for majority (solid line) and minority (dashed line) spins in one inset and the quasiparticle density-of-states in the other inset. [$P_{Mn}(n)$ is normalized so that the sum of $\int dn P_{Mn}(n)$ for majority and minority spins is equal to the total number of Mn in the simulation cell. Hole density n is measured in units of N_h/L^3, where N_h is the total number of holes in the simulation cell]. For this case the hole density at an isolated Mn is 1.63 times larger than the average hole density. The density of states $D(E)$ is per occupied hole with energies in eV. Note the anomaly at the Fermi-energy E_F, indicated by a vertical line (The choice of the zero of E is arbitrary). The number of disorder realization is fifteen for $D(E)$ and ten for $f(T)$ and $P_{Mn}(n)$. A simulation cell of side $L=8$ nm was used for these calculations. Lower panel, as in the upper panel but for the insulating case. ($N_{Mn}=0.25\ \mathrm{nm}^{-3}$ and $n_h=N_{Mn}/10$). The hole density at an isolated Mn site is 19.9 times larger than the average hole density in this case.

ent temperature dependence,[30] the exchange mean-field distribution has a well-defined maximum at strong couplings and few weakly coupled moments. Our results likely overestimate the degree of density variation in samples with $x\sim 0.05$, both because we have neglected Mn acceptor-antisite correlations[22] and because of our use of the Hartree-Fock approximation. (The corresponding self-consistent Hartree calculations lead to more sharply peaked Mn site majority-spin-density distributions.) We note that the most likely hole density at an Mn site is ≈ 1.5 times larger than the average hole density and that the most likely mean-field coupling strengths are again somewhat larger than the uniform hole-fluid value $H_{fl}=n_hJ_{pd}/2\approx 190$ K.

C. Spin stiffness

There are important differences between metallic and insulating cases in the physics that controls T_c. The metallic T_c can be limited either[29,26] by the system's stiffness against collective magnetization orientation variation or, if the stiffness is large enough, by the competition between local-moment entropy, exchange interactions, and the band energy cost of hole-spin polarization that is captured by the hole-fluid mean-field-theory T_c expression.[27,30] We have estimated the magnetic stiffness of both insulating and separations by evaluating the HF electronic energy cost of an imposed spin wave with wave-vector Q. If disorder were neglected, the procedure we follow in evaluating spin-wave energies would differ from the theory[28] of König, Lin, and MacDonald only through retardation effects. This calculation uses the semiclassical property that the quantum spin-wave energy is equal to the change in energy divided by the change in spin-polarization projection along the order-parameter direction. The wave-vector dependent quantity that we evaluate below is not an elementary excitation energy in the presence of disorder because the spin waves are no-longer plane waves, and should be thought of instead as an average of disordered spin-wave excitations weighted by the projection of the true elementary excitations onto particular plane waves. Our intention here is to provide a qualitative comparison of typical long-wavelength magnetic excitation energies in metallic and insulating limits.

In the imposed spin-wave state the orientation of a Mn spin at site $\vec{R}_I$ is $\vec{S}(\vec{Q},\vec{R}_I)=S[a\cos(\vec{Q}\cdot\vec{R}_I),a\sin(\vec{Q}\cdot\vec{R}_I),\sqrt{1-a^2}]$, where a is the spin-wave amplitude. The total HF electronic energy consistent with this Mn spin configuration is

$$E[\vec{S}(\vec{Q},\vec{R}_I)]=\sum_{\alpha=1}^{N_h} n_\alpha\epsilon_\alpha^{HF}-\frac{1}{2}\sum_{\alpha,\beta=1}^{N_h} n_\alpha n_\beta[\langle\alpha,\beta|V|\alpha,\beta\rangle - \langle\alpha,\beta|V|\beta,\alpha\rangle]. \tag{4}$$

The second term represents the total Hartree energy

$$\sum_{\alpha,\beta=1}^{N_h} n_\alpha n_\beta\langle\alpha,\beta|V|\alpha,\beta\rangle = \sum_{\sigma,\sigma'}\sum_{\vec{k}_1\vec{k}_2\vec{k}_3}\frac{4\pi e^2}{\epsilon|\vec{k}_1-\vec{k}_3|}\rho_{\vec{k}_3\sigma,\vec{k}_1\sigma}\rho_{\vec{k}_1+\vec{k}_2-\vec{k}_3\sigma',\vec{k}_2,\sigma'} \tag{5}$$

and the last term represents the total exchange energy

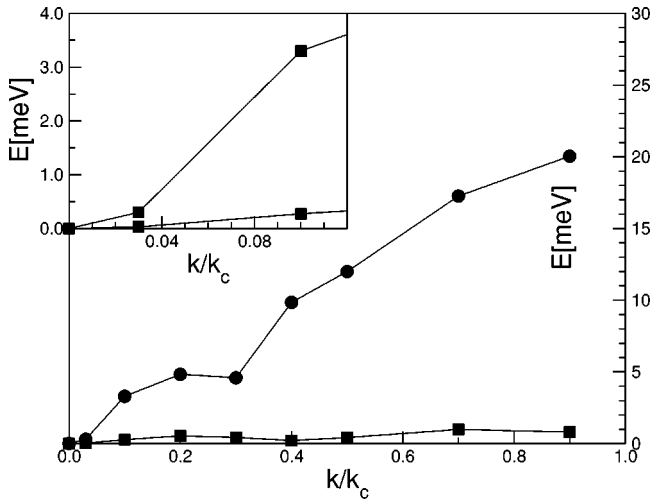

FIG. 3. Average spin-flip energy vs wave vector. The upper curve is for the metallic case while the lower curve is for the insulating case. The wave vector is normalized to a Debye wave vector defined by the Mn density in each case, $k_c=(6\pi^2 N_{Mn})^{1/3}$. The inset shows a magnified view of in the small wave vector regime. These results demonstrate that the spin stiffness is substantially smaller in the insulating case.

$$\sum_{\alpha,\beta=1}^{N_h} n_\alpha n_\beta \langle \alpha,\beta|V|\beta,\alpha\rangle$$

$$= \sum_{\sigma,\sigma'} \sum_{\vec{k}_1\vec{k}_2\vec{k}_3} \frac{4\pi e^2}{\epsilon|\vec{k}_1-\vec{k}_3|} \rho_{\vec{k}_1+\vec{k}_2-\vec{k}_3\sigma',\vec{k}_1,\sigma} \rho_{\vec{k}_3\sigma,\vec{k}_2\sigma'} . \quad (6)$$

Figure 3 displays average spin reversal energy, defined as the energy change divided by the change in total spin, for metallic and insulating states. Note that the energy cost of slow (long wavelength) spin-direction variations is extremely small in the insulating case because of the relatively weak magnetic between magnetic polarons that establish long-range magnetic order. It follows that the hole-fluid mean-field will completely fail in estimating the critical temperature of insulating DMS ferromagnets. The energy cost for spin-direction variations that we find in the metallic case is in qualitative agreement with hole-fluid model results, although it is larger at short wavelengths. In the hole-fluid mean-field theory the energy cost of spin-direction variations would equal H_{fl} at all wave vectors. It follows that for the parabolic band model we have studied substantial corrections[29,26] would apply to its mean-field T_c. It is important to note, however, that valence-band spin-orbit interactions stiffen collective spin variations in these ferromagnets,[30] reducing corrections to mean-field-theory T_c estimates.

IV. SUMMARY

It is generally accepted that ferromagnetism in (III,Mn)V diluted magnetic semiconductors is due to coupling between the orientations of Mn ion local moments by holes in the semiconductor valence band. Ferromagnetism in these systems is often discussed using one or the other of two extreme models, which are intended for the cases of weakly disordered holes and localized holes, respectively. The key approximation of the first approach is that disorder in the magnetically doped semiconductor is either ignored or treated perturbatively, while the key approximation of the second approach is that the holes are assumed to be strongly localized in approximately hydrogenic wave-functions bound to Mn acceptors. In this paper, we have numerically studied a more general model using a Hartree-Fock approximation that captures the physics of both limits. The numerical results presented here are for two cases, $x=0.0125$ with strongly compensated Mn acceptors and $x=0.05$ with more weakly compensated Mn acceptors. Ferromagnetism occurs in both circumstances experimentally, although with a much lower transition temperature in the former case, while transport measurements show insulating behavior at the lower Mn fraction and metallic behavior at the higher Mn fraction. In order to characterize the nature of the ferromagnetic ground state we have evaluated the strength of the mean-field exchange interaction between Mn ions and valence-band holes at each Mn site. In the insulating case we find that a relatively small fraction of the Mn ions are strongly coupled to valence band holes. This result is consistent with a magnetic polaron picture[13] of ferromagnetism in the insulating regime, although quantitative aspects of this result show that naive application of a hydrogenic wave-function model cannot yield quantitative accuracy. For the *metallic* case, we demonstrate that all Mn ions are strongly coupled to valence-band holes and that the typical coupling strength is close to that of the uniform density hole-fluid model. There is, however, still considerable variation in the coupling strength which creates a random potential for both majority and minority spins. This potential variation contributes importantly to current relaxation and helps limit[31] the conductivity of metallic samples. Unlike typical ferromagnets, scattering from the order parameter is important for transport properties even at $T=0$. Our results suggest that a weak-coupling treatment of disorder is reliable for strongly metallic (III,Mn)V ferromagnet samples.

ACKNOWLEDGMENTS

SREY is supported in part by the KOSEF Quantum-functional Semiconductor Research Center at Dongkuk University. Work at the University of Texas was supported by the Welch foundation and by DARPA/ONR Grant No. N00014-00-1-095.

[1] H. Ohno, J. Magn. Magn. Mater. **200**, 110 (1999) and work cited therein; M.L. Reed, N.A. El-Masry, H.H. Stadelmaier, M.K. Ritums, M.J. Reed, C.A. Parker, J.C. Roberts, and S.M. Bedair, Appl. Phys. Lett. **79**, 3473 (2001); Y.D. Park, A.T. Hanbicki, S.C. Erwin, C.S. Hellberg, J.M. Sullivan, J.E. Mattson, T.F. Ambrose, A. Wilson, G. Spanos, and S.T. Jonker, Science **295**, 651 (2002); T. Slupinski, H. Munekata H, and A. Oiwa, Appl. Phys. Lett. **80**, 1592 (2002); X. Chen, M. Na, M. Cheon, S. Wang, H.

Luo, B.D. McCombe, X. Liu, Y. Sasaki, T. Wojtowicz, J.K. Furdyna, S.J. Potashnik, and P. Schiffer, Appl. Phys. (N.Y.) **81**, 511 (2002); N. Theodoropoulou, A.F. Hebard, M.E. Overberg, C.R. Abernathy, S.J. Pearton, S.N.G. Chu, and R.G. Wilson, Phys. Rev. Lett. **89**, 107203 (2002).

[2] H. Munekata, H. Ohno, S. Vonmolnar, A. Segmuller, L.L. Chang, and L. Esaki, Phys. Rev. Lett. **63**, 1849 (1989); H. Ohno, H. Munekata, T. Penney, S. von Molnar, and L. Chang, *ibid.* **68**, 2664 (1992).

[3] J. König, J. Schliemann, T. Jungwirth, and A. H. MacDoanld, in *Electronic Structure and Magnetism of Complex Materials*, edited by D. J. Singh and D. A. Papaconstantopoulos (Springer-Verlag, Berlin 2002); J. König, J. Schliemann, T. Jungwirth, and A.H. MacDoanld, also available at cond-mat/0111314 (unpublished).

[4] J. Szczytko, A. Twardowski, K. Swiatek, M. Palczewska, M. Tanaka, T. Hayashi, and K. Ando, Phys. Rev. B **60**, 8304 (1999).

[5] M. Linnarsson, E. Janzen, B. Monemar, M. Kleverman, and A. Thilderkvist, Phys. Rev. B **55**, 6938 (1997).

[6] O.M. Fedorych, E.M. Hankiewicz, Z. Wilamowski, and J. Sadowski, Phys. Rev. B **66**, 045201 (2002).

[7] H. Ohno, Science **281**, 951 (1998).

[8] F. Matsukura, H. Ohno, A. Shen, and Y. Sugawara, Phys. Rev. B **57**, R2037 (1998).

[9] T. Hayashi, Y. Hashimoto, S. Katsumoto, and Y. Iye, Appl. Phys. Lett. **78**, 1691 (2001).

[10] S.J. Potashnik, K.C. Ku, S.H. Chun, J.J. Berry, N. Samarth, and P. Schiffer, Appl. Phys. Lett. **79**, 1495 (2001); S.J. Potashnik, K.C. Ku, R. Mahendiran, S.H. Chun, R.F. Wang, N. Samarth, and P. Schiffer, Phys. Rev. B **66**, 012408 (2002); K.W. Edmonds, K.Y. Wang, R.P. Campion, A.C. Neumann, C.T. Foxon, B.L. Gallagher, and P.C. Main, Appl. Phys. Lett. **81**, 3010 (2002).

[11] T. Jungwirth, W.A. Atkinson, B.H. Lee, and A.H. MacDonald, Phys. Rev. B **59**, 9818 (1999); T. Jungwirth, J. Konig, J. Sinova, J. Kucera, and A.H. MacDonald, *ibid.* **66**, 012402 (2002).

[12] M. Berciu and R.N. Bhatt, Phys. Rev. Lett. **87**, 107203 (2000); Adam C. Durst, R.N. Bhatt, and P.A. Wolff, Phys. Rev. B **65**, 235205 (2002).

[13] A. Kaminski and S. Das Sarma, Phys. Rev. Lett. **88**, 247202 (2002).

[14] C. Timm, F. Schäfer, and F. von Oppen, Phys. Rev. Lett. **89**, 137201 (2002).

[15] T. Dietl, H. Ohno, F. Matsukura, J. Cibert, and D. Ferrand, Science **287**, 1019 (2000); T. Dietl, H. Ohno, and F. Matsukura, Phys. Rev. B **63**, 195205 (2001).

[16] M. Abolfath, T. Jungwirth, J. Brum, and A.H. MacDonald, Phys. Rev. B **63**, 054418 (2001).

[17] The carrier density in annealed samples at $x=0.05$ has been extracted from high-field Hall effect data by T. Omiya, F. Matsukura, T. Dietl, Y. Ohno, T. Sakon, M. Motokawa, and H. Ohno, Physica E **7**, 976 (2000). The degree of compensation at $x=0.01$ is less accurately known and likely to be sample dependent.

[18] Density-functional electronic-structure techniques have been applied to these materials and will be important in refining models of the type we study. This approach has not yet advanced sufficiently to address the questions of interest here, partly because the local-density approximation overestimates exchange-coupling strengths. For a review see S. Sanvito, G. Theurich, and N.A. Hill, cond-mat/0111300 (unpublished).

[19] J. Schliemann and A.H. MacDonald, Phys. Rev. Lett. **88**, 137201 (2002), have suggested that noncollinear ground-state Mn ion orientations can occur in models with kinetic exchange only. Our calculations demonstrate that Coulomb interactions favor collinear configurations, although noncollinear configurations are still likely in the insulating regime. Quantum fluctuations in Mn ion orientations are weak because of the large separation between the energy scales for band electron and Mn ion spin fluctuations.

[20] A.K. Bhattacharjee and C. Benoit à la Guillaume, Solid State Commun. **113**, 17 (2000).

[21] Gergely Zarand and Boldizsar Janko, Phys. Rev. Lett. **89**, 047201 (2002).

[22] C. Timm, F. Schäfer, and F. von Oppen have pointed out that defect correlations, which we do not include here, will reduce the importance of disorder, expanding the validity range of the hole-fluid picture.

[23] The model Hamiltonian parameters we use are those generally accepted for (Ga,Mn)As, the best understood (III,Mn) V ferromagnet. $J_{pd}=0.1$ eV nm^3, $a_0=0.3$ nm, $\epsilon=10$, $V_0=2.5$ eV and $r_0=0.259$ nm. We diagonalize the HF Hamiltonian in a plane-wave representation, using periodic boundary conditions in the simulation cell. For different system sizes we maintain the cutoff wave-vector $k_{max}=\pi$ nm^{-1}.

[24] S.-R. Eric Yang and A.H. MacDonald, Phys. Rev. Lett. **70**, 4110 (1993); S.-R. Eric Yang, A.H. MacDonald, and B. Huckestein, *ibid.* **74**, 3229 (1995); S.-R. Eric Yang, Ziqiang Wang, and A.H. MacDonald, Phys. Rev. B **65**, 041302 (2001).

[25] K.C. Ku, S.J. Potashnik, R.F. Wang, M.J. Seong, E. Johnston-Halperin, R.C. Meyers, S.H. Chun, A. Mascarenhas, A.C. Gossard, D.D. Awschalom, P. Schiffer, and N. Samarth, cond-mat/0210426 (unpublished); K.W. Edmonds, K.Y. Wang, R.P. Campion, A.C. Neumann, N.R.S. Farley, B.L. Gallagher, and C.T. Foxon, cond-mat/0209554 (unpublished).

[26] A. Chattopadhyay, S. Das Sarma, and A.J. Millis, Phys. Rev. Lett. **87**, 227202 (2001).

[27] T. Dietl, A. Haury, and Y. M dAubigne, Phys. Rev. B **55**, R3347 (1997).

[28] J. König, H.H. Lin, and A.H. MacDoanld, Phys. Rev. Lett. **84**, 5628 (2000).

[29] J. Schliemann, J. Konig, H.H. Lin, and A.H. MacDonald, Appl. Phys. Lett. **78**, 1550 (2001); J. Schliemann, J. König, and A.H. MacDonald, Phys. Rev. B **64**, 165201 (2001).

[30] J. König, T. Jungwirth, and A.H. MacDonald, Phys. Rev. B **64**, 184423 (2001).

[31] T. Jungwirth, M. Abolfath, Jairo Sinova, J. Kucera, A.H. MacDonald, cond-mat/0206416 (unpublished).